Optical position detection to measure tyre carcass deflections

A.J. Tuononen*

Helsinki University of Technology, Laboratory of Automotive Engineering, TKK, Finland

Active safety systems would benefit from tyre force and friction potential information. Different sensor concepts, including, among others, the EU–funded Apollo–project developed tyre sensor based on optical position detection, are being studied. The sensor can measure tyre carcass deflections with respect to the rim. The carcass deflections can be used to calculate tyre forces and they may be exploited in the estimation of friction potential. The waveforms of the sensor signal are illustrated. The vertical and lateral force estimations are presented with unavoidable compensation parts. The tyre sensor measurements were compared to the measurement–vehicle results and good correlations achieved. Continuing activities are concerned with the estimation of friction potential and the detection of aquaplaning.

Keywords: tyre sensor; tyre force estimation; optical position detection

1. Introduction

Estimation of tyre forces and friction potential could improve the performance of the active safety systems that have rapidly become common equipment in all vehicle categories. In practice, almost all the forces and moments acting on a vehicle are generated by the tyres. In addition, tyre characteristics dominate the vehicle response. These are naturally reasons why many involved in developing active safety systems are interested in tyre sensors.

Tyre sensors can be used for various purposes and a number of different technologies are being studied. To clarify this, tyre sensors can be divided into groups depending on function and technology. The different functions for the tyre sensors could be:

- estimation of friction potential;
- estimation of tyre forces (used friction);
- estimation of wheel speed, slip ratio and slip angle;
- tyre pressure monitoring;
- recognition of tyre wearing, imbalance etc., and
- recognition of worn suspension components (mostly heavy vehicles).

*Email: ari.tuononen@tkk.fi

Even though intensive research is being conducted in some of these areas, only tyre pressure monitoring systems are available on the market.

If tyre forces and friction potential are the main interest, the following technologies could come into question:

- measuring forces and moments from suspension parts [1];
- measuring deflection of wheel [2];
- measuring tyre deflections with sensor in suspension [3,4] and
- sensor in tyre [5–9].

It is possible to measure tyre forces and moments from suspension parts. Furthermore, the relation of lateral force and aligning moment can be used to estimate friction potential and slip angle [1]. However, some lateral force is needed for estimation.

As well as the suspension parts, the rim can be used for force and moment estimation [2]. The important difference is that the wireless data transmission is needed from the rotating rim and this makes the setup more expensive and complicated. It is also questionable whether it can produce any information in addition to that gained from a measurement setup in the suspension.

A tyre carcass is deflected under vertical, lateral and longitudinal forces; there are several approaches to measuring such deflections. The Continental Side Wall Torsion (SWT) sensor [3] seemed really promising when it was first presented. However, due to the fact that SWT has not appeared in production, it is possible that, even if the tyre forces could be accurately measured, the ABS/ESP system would not be of sufficient benefit to justify the costs of such system.

The type of tyre sensor that measures tyre tread deformation is probably the most interesting. Darmstadt Technical University has studied this area carefully since 1988 [5,10]. Atyre tread deformation sensor can yield information on the coefficient of friction, on tyre forces (X, Y, Z), the risk of hydroplaning, tyre temperature and tyre pressure [11].

Bridgestone has been developing both acceleration and strain tyre sensors. They call their concept 'Contact area information sensing' (CAIS). The strain sensor is used to calculate the lateral force, wheel load, camber angle and slip angle. The acceleration sensor is for road condition characterisation. The most interesting part, the friction estimation algorithm, is based on the phenomenon of the movement of the tread block being larger on a low friction surface [8].

Thus, the strain monitoring of the tyre might be key to the friction potential estimation. Passive sensors would solve the energy problem in the tyre and an interesting approach is presented in ref. [4]. They propose that a tyre structure with an electrically conductive steel belt and dielectric rubber is quite similar to an electrical condenser. Thus, the tyre capacitance change and tuning frequency indicates the tyre strain or deformation, so sensors are not needed in the tyre. The major observation is that the capacitance of the tyre increases with an increase in tensile loading.

A Surface Acoustic Wave (SAW) sensor is adapted to measure the movement of the tread block in ref. [9]. A pin is inserted through the belt, while the sensor is in the inner liner of the tyre. The movement of the pin bends the SAW-sensor. The sensor's response to a radio request signal can be used to evaluate the deformation of the tread. The SAW-sensor is passive, thus there is no need for energy.

The APOLLO-project 2002–2005 developed the 3-in-l intelligent tyre. This consists of three different types of sensors in the same tyre to make the comparison of sensors as effective as possible. The acceleration sensor and strain sensor showed potential, but the durability problems made

these approaches less attractive. Meanwhile, an optical sensor that can measure carcass deflections was simple and practical and indicated potential for tyre force estimation [6,7].

If the optical sensor could measure the aligning moment of the tyre as well, it would provide an opportunity for friction potential estimation (cf. [1]). Another possibility for friction potential estimation is to detect influence of stress distribution along the contact patch from measured carcass deflections. This would offer friction potential estimation from free rolling tyre. In addition, aquaplaning detection and tyre pressure monitoring are obvious and realistic functions for optical tyre sensors.

This paper introduces the principle of the optical tyre sensor and algorithms that are needed for tyre force calculations.

2.   Optical tyre sensor

The core of the optical tyre sensor is a two-dimensional position sensitive detector (PSD) that utilises photodiode surface resistance. The PSD is located on the rim and can detect the movement of a light emitting diode (LED) that is installed in the inner liner of the tyre (Figures 1–3). Note that the intensity of the LED is not constant versus angular displacement. For example, a 30° angular displacement means 20% lower intensity.

The Piano-Convex (PCX) Lens with anti-reflection coating is used to focus the light to the sensor. The effective focal length is 9 mm, which is also the distance of the lens from the sensor.

The sensor setup has been installed into a special dividable rim; the tyre in these tests was a winter tyre without studs (friction tyre, 225/60R16). A LiIon-battery was used as a power supply. The data from the sensor was digitized and transmitted wirelessly to the receiver at 433 MHz. The resolution of the data was 12 bits and the sampling rate was 3105 Hz. The data was transformed for CAN-message format to be ready for the vehicle network.
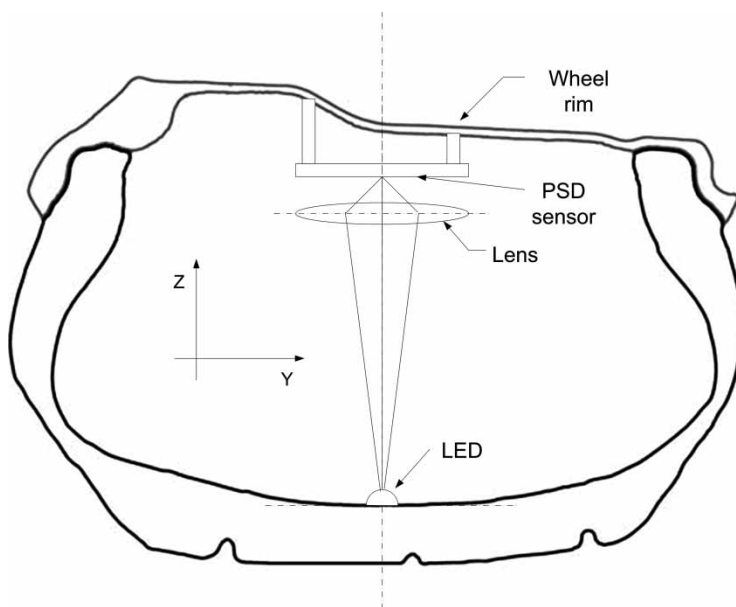

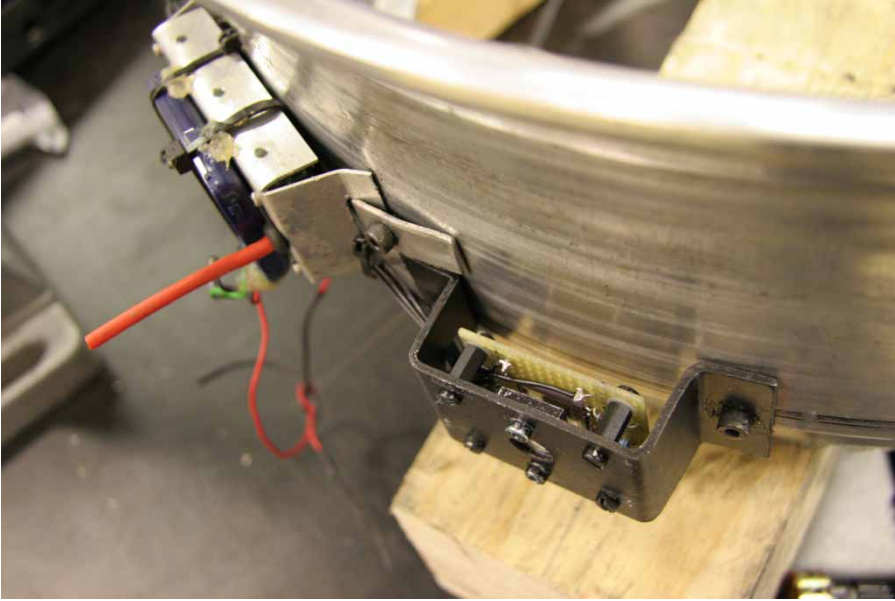Figure 1.   Cross-section of tyre sensor assemblage.

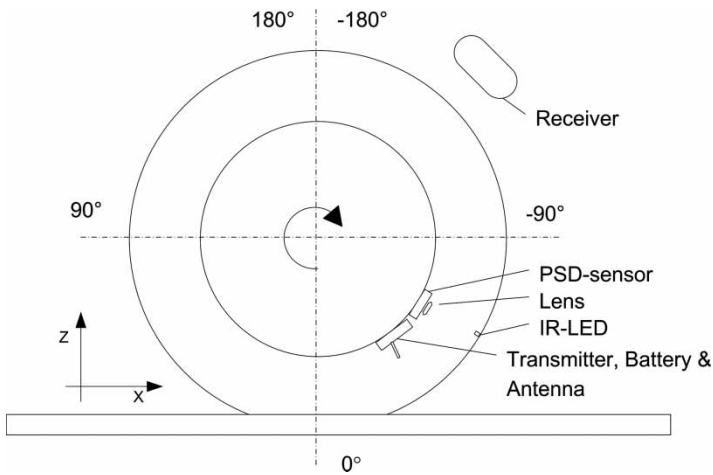Figure 2.   Optical sensor with lens (right) and transmitter (left).

Figure 3.   Optical tyre sensor components.

The output of PSD is four channels and the manufacturer [12] gives the following equations to calculate the position of the light spot on the sensor surface:

$$x = \frac{L}{2} \frac{(i_{x2} + i_{y1}) - (i_{x1} + i_{y2})}{i_{x1} + i_{x2} + i_{y1} + i_{y2}} \tag{1}$$

$$y = \frac{L}{2} \frac{(i_{x2} + i_{y2}) - (i_{x1} + i_{y1})}{i_{x1} + i_{x2} + i_{y1} + i_{y2}} \tag{2}$$

$$z = \sqrt{\frac{1}{i_{x1} + i_{x2} + i_{y1} + i_{y2}}} \tag{3}$$

where i_{x2}, i_{x1}, i_{y1} and i_{y2} are measured photocurrents from the sensor output electrodes. The size of the sensor is taken into account by length of the active area L (10 mm).

A tyre measurement vehicle was used to measure slip angle, slip ratio, wheel speed, tyre forces and moments. The vehicle was a light truck with 'fifth' wheel, where the measurement hub was installed. The surface was a tarmac highway [13].

Laboratory measurements were performed in a tyre test rig over the chassis dynamometer drum covered with Safety-Walk™ -paper [14]. Due to the complexity of analysing the influence of a small-diameter drum (1219 mm), the measurement vehicle results are presented in this paper, if not otherwise stated. However, the tyre test rig had a major role in developing real-time data transmission and analysis.

Data acquisition systems were separate for the tyre sensor and measurement vehicle. Hence, the exact synchronisation of the data is virtually impossible in the post-processing phase. This means that there is no possibility of drawing a conclusion about the response time of the optical tyre sensor. The rise time of the PSD-sensor is two microseconds [12].

3. Measurements

Vertical displacement of the LED with different wheel loads is shown in Figure 4. Velocity was 30 km/h in all the measurements. It can be seen that there is variation in the peak values and in the shape before and after contact as well. Figure 3 clarifies the direction of rotation and sensor position angle (abscissa).

The vertical displacement signal is used to synchronise the sensor position. The peak value is detected and stands for a 0° angle; at this moment the sensor points directly downwards to the road.

Longitudinal displacement in free rolling with different wheel loads is shown in Figure 5. The scale of the y-axis is given, but is only indicative. Before the contact begins, the LED is forced to move due to the compressive pressure from contact deformation. This same phenomenon can be seen after the contact (positive angles), but naturally displacement is in the other direction. The longitudinal displacement is zero when the sensor position is approximately down or up (0 or + −180°). During the contact, the LED is moving rapidly from peak-to-peak. The peak values are
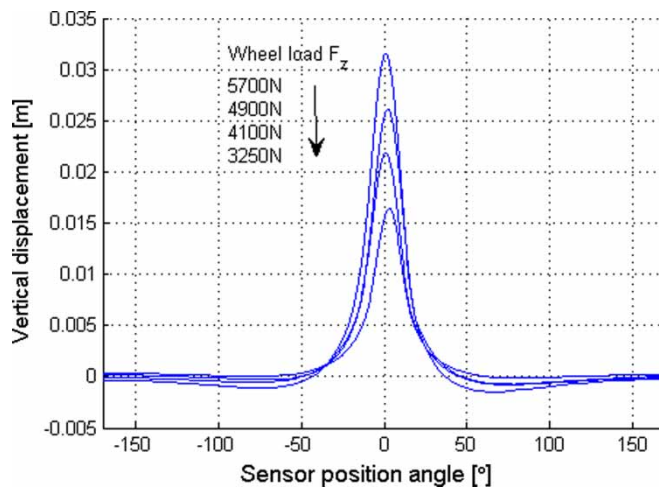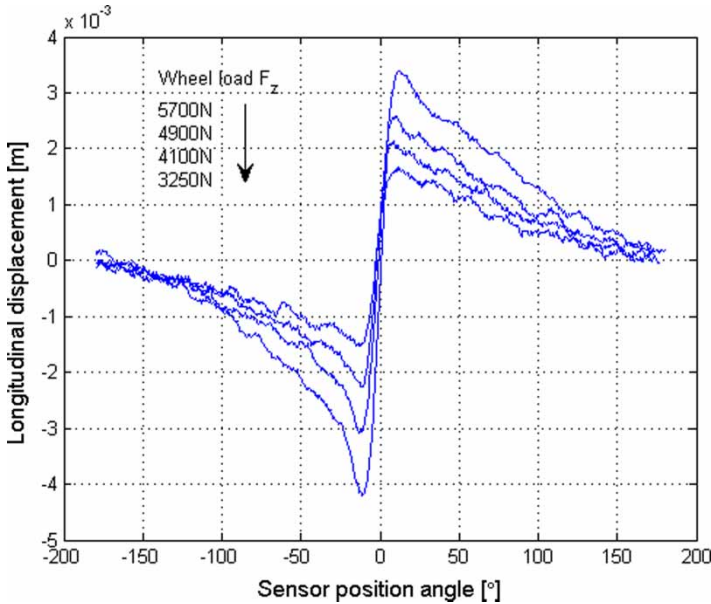

Figure 4. Vertical displacement of LED.

Figure 5.   Longitudinal displacement of LED.

not the same before and after contact. This is supposed to be the result of a slight alignment error between the rim, sensor and lens. This was confirmed with static measurement.

The sensor can also measure lateral displacement of the LED. Obviously, some movement should be detected when the tyre is under lateral force. Therefore, during free rolling there should not be any noticeable lateral movement. However, it is practically impossible to install the LED exactly centred to the sensor. This means that there is some lateral offset error that has to be compensated. When the distance of the LED to the sensor is constant, the offset error remains constant as well. Unfortunately, during the contact, the LED moves closer to the sensor and the lateral position of the light spot reflected from the lens is moving, even though the LED stays still laterally (Figure 6). This movement can be compensated as shown in the following equation:

$$y = y_{\text{raw}} - y_0 \left(\frac{z - z_0}{z_0} k_z + 1 \right) \tag{4}$$

where y_{raw} is lateral displacement, y_0 is installation offset error, z is vertical displacement, z_0 is unloaded vertical displacement and k_z is the constant that describes the relation of signal and actual movement of the LED. The compensated and original signal with different vertical load can be seen in Figure 7. The influence of lateral installation offset can be removed from the signal almost completely.

The lateral displacement of the LED during rotation with different slip angles can be seen in Figure 8. Displacement is increasing with slip angle, but non-linearly. This can be explained by the tyre forces that the particular slip angle is generating. There is not such a great difference between tyre forces between slip angles 6° and 8° as between those of 2° and 4°.

The response for vertical load steps can be seen in Figure 9. The forces from the tyre sensor are calculated once in rotation. The equation proposed for vertical force is:

$$F_z = k_{Fz} \int_{-180°}^{180°} (z - z_o) \mathrm{d}\varphi \tag{5}$$
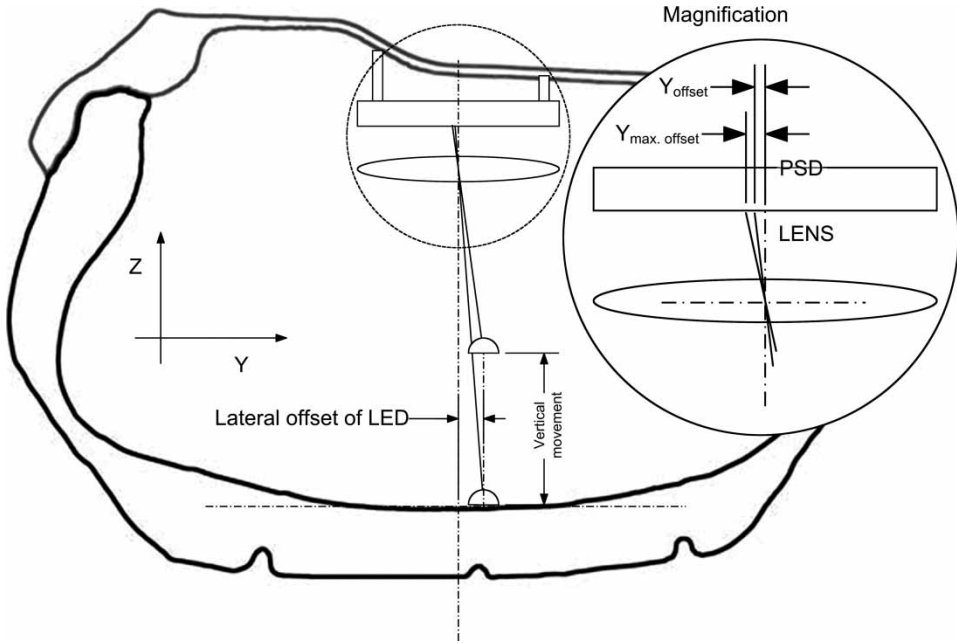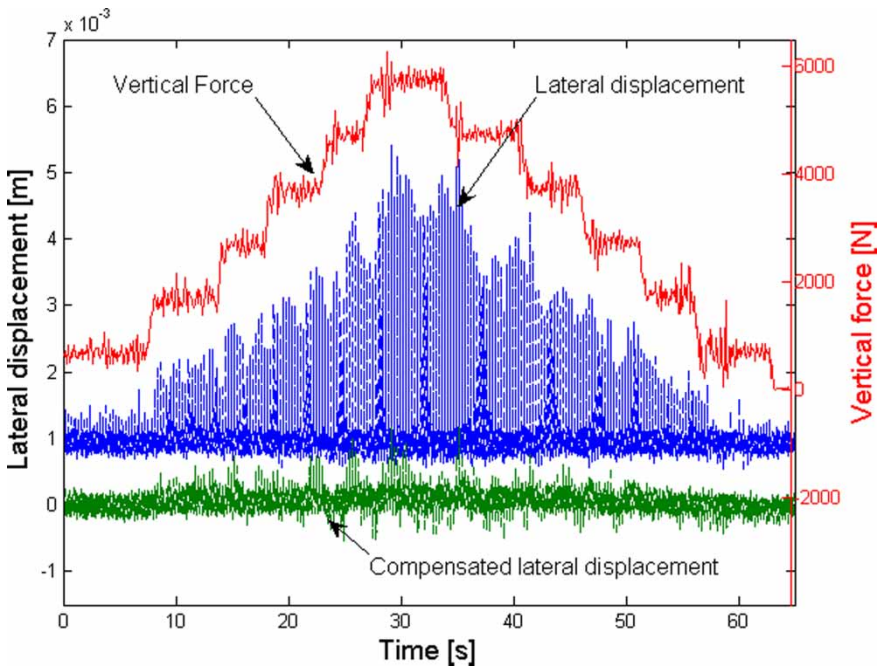
Figure 6.   Lateral offset during vertical movement.

Figure 7.   Influence of vertical force for lateral displacement and compensated signal (slip angle 0°).

where z is the vertical displacement signal and z_0 is z-value in unloaded situation. The area of the vertical displacement curve is multiplied by constant k_{Fz}; note that this is not equal to the vertical stiffness of the tyre.
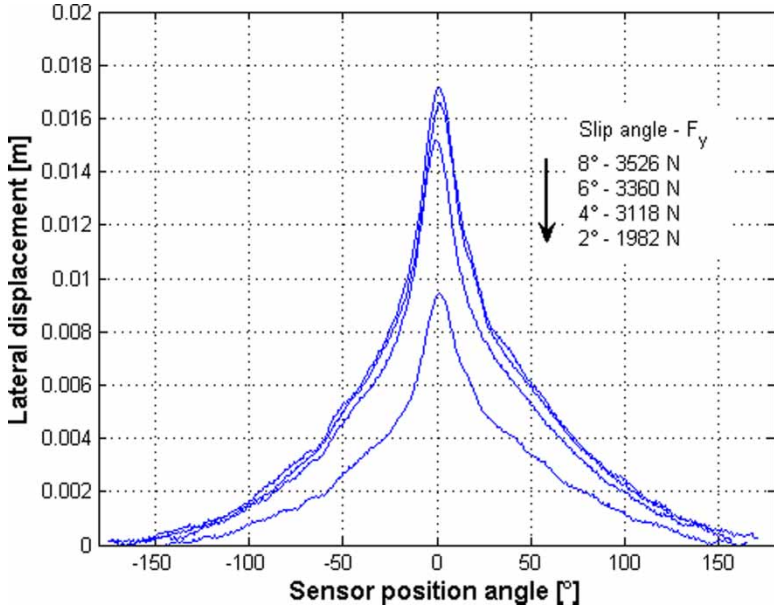
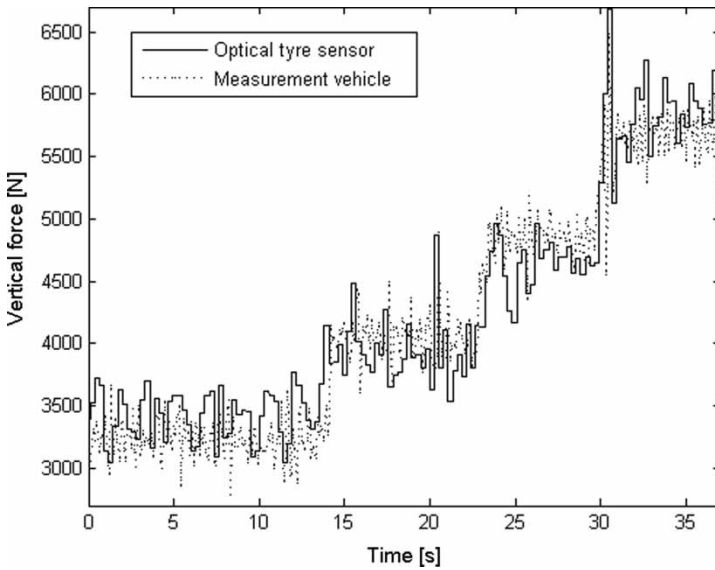Figure 8. Lateral displacement of LED at different slip angles.

Figure 9. Comparison of vertical force from test vehicle force hub and tyre sensor.

The lateral force is calculated in a way similar to vertical force, but naturally it is based on the y-signal. The lateral force can be calculated:

$$F_y = k_{Fy} \int_{-180°}^{180°} y \, d\varphi \qquad (6)$$
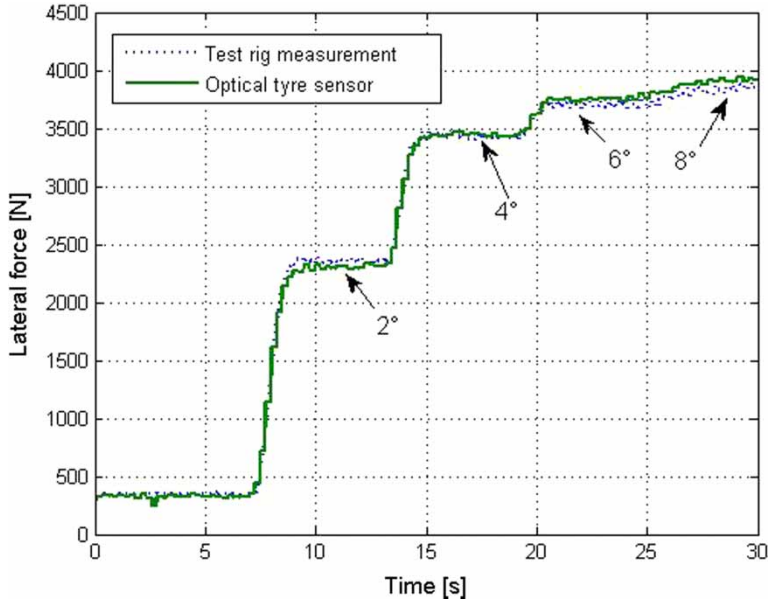
The comparison is presented in Figure 10.

Figure 10.   Comparison of lateral force from test rig and tyre sensor.

The constants k_{Fy} and k_{Fz} correlate strongly with inflation pressure, which in turn depends on temperature of the air. In consequence, the inflation pressure has to be measured in order have reliable estimate for tyre forces in all conditions.

4.   Discussion

The vertical force from the optical sensor and from the measurement vehicle shows good correlation. The equation was presented to calculate wheel load, but other methods exist as well. For example, the peak of the z-signal increases quite linearly with wheel load, but is probably more sensitive to errors in the signal than the presented method.

Unfortunately, the z-signal is influenced by the error from the angular movement of the LED (Figure 1), which cannot be ignored. The intensity of the LED depends on the angle of the LED to the sensor. The intensity is decreased when the LED is rotated away from 0° angle. This mainly has an influence on the measured intensity, z-signal. The angular movement is greatest in the situation when the LED enters and leaves the contact. Thus, the vertical displacements curves are slightly too slim, but the peak value is not disturbed by this phenomenon. The longitudinal (x-signal) and lateral (y-signal) are not greatly affected by the angular movement of the LED, because the influence of intensity is simply compensated as shown in Equations 1 and 2 (dividing by the sum of all signals).

The longitudinal signal offers the potential to calculate longitudinal forces. This is possible by calculating the shift of the x-signal in the contact centre. However, during ABS-braking, the brake pressure is varied at such a high frequency that a 'once-per-rotation'-based force calculation does not necessarily work. Moreover, the brake pressure or engine torque can be exploited to estimate longitudinal tyre forces, as obviously done in existing stability control systems. It is also questionable, are the braking forces needed at all, if the friction potential would be available before the full braking is applied. The ABS-algorithm could select suitable control parameters according to the friction conditions.

The lateral force calculated from the optical sensor showed a really good correlation to the test-rig measurement. It would be interesting to calculate the aligning moment as well, because the peak value of the y-signal is slightly behind the contact centre and is proposed to be due to the influence of the pneumatic trail. The reliable measurement of the pneumatic trail could provide the possibility of estimating friction potential. However, highly accurate and reliable rotation angle recognition is needed before such results can be presented. On the other hand, the tyre force calculations are not sensitive for rotation angle recognition, because the values of deflections are minor when the integrator is reset in Equations 5 and 6. Meanwhile, the reliability of contact recognition is vital. If the contact recognition misses the contact, the algorithm would sum the deflections of several rotations, and thus the force estimate diverges instantly.

The optical tyre sensor, among other devices, has proven to be representative of an interesting approach, with its benefits and imperfections. It is a little premature to say that it has enough potential to become a product, however. In practice, the biggest barrier to that may be the fact that the tyre can move on the rim, and after one hard braking, the LED is no longer in the same position as the PSD-sensor. Equally, the LED in the inner liner has to be connected to the rim with limited-length wires. Thus, the tyre has to be fixed to the rim, which is not necessarily an easy task for mass production.

It can be seen that tyre sensor research is dividing in two directions: towards the sensors that offer the possibility of studying the friction phenomena and towards the sensors that are financially profitable in mass production. The passive sensors are of interest, but the measured phenomenon is distant from tyre friction. Even though the passive sensors show some consistent trends in laboratory tests, a lot of work has still to be done before sensors work reliably in all extreme conditions that a tyre can face. On the other hand, active tread deformation sensors can be easily used for friction estimation, but the durability and energy problems stay unsolved.

However, both approaches can improve the knowledge of tyre behaviour. Perhaps the algorithms for friction estimation can be developed with simple strain or movement sensors in research tyres. Such developed algorithms can be further used to develop cheap and durable passive tyre sensors.

Acknowledgements

References

[1] W.R. Pasterkamp, *The Tyre as Sensor to Estimate Friction*, Delft University Press, 1997.
[2] M. Gobbi and G. Mastinu, *Wheels with Integrated Sensors for Measuring Tyre Forces and Moment*, AVEC, 2004.
[3] T. Becherer, *The sidewall torsion sensor system, VDI-Fortschirittberichte*, Reihe 12, pp. 362.
[4] R. Matsuzaki and A. Torodoki, *Passive strain monitoring of tyres using capacitance and tuning frequency changes*, Smart Mater. Struct. 14 (2005), pp. 561–568.
[5] B. Breuer, U. Eichhorn, and J. Roth, *Measurement of Tyre/road-Friction Ahead of the Car and Inside the Tyre*, AVEC, 1992.
[6] APOLLO, Final report, Available online at: www.vtt.fi/apollo
[7] J. Holtschulze, H. Goertz, and T. Husemann, *A simplified tyre model for intelligent tyres*, Veh. Sys. Dyn. 43 (suppl), pp. 305–316.
[8] H. Morinaga, *Development of Sensing Algorithm for Intelligent Tire*, Tire Technology Expo, 2006.
[9] A. Pohl, R. Steindl, and L. Reindl, *The intelligent tire utilizing SAW sensors – measurement of tire friction*, IEEE Trans. Instrument. Measure. 48(6) (1999), pp. 1041–1046.
[10] O. Yilmazoglu et al., *Integrated InAs/GaSb 3D magnetic field sensors for "the intelligent tire"*, Sensors and Actuators A 94 (2001), pp. 59–63.
[11] S. Gruber et al., *Elements of a mechatronic vehicle corner*, Mechatronics 12 (2001), pp. 1069–1080.

[12] Hamamatsu™, PSD S5991-01 data sheet.

[13] J. Hakanen and T. Kähärä, *Tyre Characterisation on Ice and Snow with a Measurement Vehicle, Friction potential and safety: prediction of handling behaviour*, 2nd International Colloquium on Vehicle Tyre Road Interaction, Florence, 2001.

[14] H. Pirjola, *Dynamic tyre force measuring device*, Helsinki University of Technology, Department of Mechanical Engineering (2002), Available at http://www.tkk.fi/Units/Auto/23.5.2006.